Molecular Dynamics Simulation of Friction in Xenon Films on a Silver Substrate

M. S. Tomassone, J. B. Sokoloff, A. Widom, and J. Krim

Department of Physics and Center for Interdisciplinary Research on Complex Systems, Northeastern University, Boston, MA 02115

(February 1, 2008)

Abstract

We perform molecular dynamics simulations of friction for atomically thin Xe films sliding on Ag(111). We determine the inverse of the coefficient of friction (i.e slip time) by direct calculation of the decay of the center of mass velocity after applying an external force, as well as from the velocity auto-correlation function. We find that the slip time exhibits a drop followed by a sharp increase in a range of coverage near one monolayer. The slip time then levels off with further coverage increases in agreement with previously reported experiments. Our simulations suggest that the friction found in this system is dominated by phonon excitations.

PACS numbers: 79.20.Rf, 64.60.Ht, 68.35.Rh

Although tribology, the study of friction and wear, has been of technological interest since ancient times [1,2], the topic continues to rouse interest today [3–12]. Rapid progress in experimental, theoretical and computational methods provides new insights into the atomic origins of frictional energy dissipation. When a thin film slides on a metal substrate there exists dissipation of energy via two mechanisms: (i) electronic excitations in the metallic substrate [4,9], and (ii) phonon excitations in the film or in the substrate [10]. The dissipation of energy can be characterized by the slip time τ (i.e. the time it takes for the film's speed to fall to $1/e$ of its original value, assuming it is stopped by friction) or equivalently by a damping coefficient $\eta \sim 1/\tau$.

In this letter we study the phonon contribution to friction for Xe films sliding along a Ag(111) substrate using molecular dynamics simulations. It is of great interest to find a way to determine the relative contributions of the phonon and electron contributions to friction, since to date it is not clear which is dominant. To this end, we compare our results with the slip-time versus coverage data reported by Daly and Krim [6], and with the electrical resistivity versus coverage data of Dayo and Krim [7]. The results of this comparison suggest that phonon excitations make a dominant contribution to the friction.

We determine the slip time as function of coverage, defined as the number of atoms in the film per unit area. We treat a range of film coverages, from submonolayer to bilayer. The slip time is determined by two methods. In the first method, an initial center of mass velocity $\mathbf{V}_0$ is produced by an external force exerted on the film for $t < 0$. The external force is turned off for $t > 0$, and τ is determined by the resulting velocity decay $\mathbf{V}_0 e^{-t/\tau}$. In the second method, no external force is applied. The slip time is determined by the behavior of the thermal equilibrium autocorrelation for the center of mass velocity as a function of time. The autocorrelation function is related to the linear response of the system to a small perturbation by Kubo theory [13]. Linear response theory [12] holds in the limit of zero driving velocity and zero response force. Therefore, this method is advantageous for describing experiments using the Quartz Crystal Microbalance (QCM) [6,8], since the QCM drives the film out of equilibrium only to a very small extent. This new method for

calculating the slip-time is more appropriate for the small sliding velocities that occur in the actual experiment than previously used methods. Previous methods apply unphysically large forces (or, alternatively, shake the substrate at unphysically high frequencies) in order to generate velocities which are several orders of magnitude larger than those which occurred in the experiment.

Molecular dynamics simulations of sliding friction have traditionally employed *thermostats* which add or remove energy to or from the system in order to achieve constant temperature. Thermostats used in molecular dynamics have the side effect of damping the atomic motions, resulting in an additional contribution to friction [11,10]. In order to study friction in a situation free of such complications, we employ a thermostat solely to establish statistical thermal equilibrium, but then turn it off while monitoring the system's properties. The absence of a thermostat in the simulation, allows us to focus exclusively on the film's dissipation due to phonons.

The model Hamiltonian for N film atoms of mass m at positions $\mathbf{r}_k$ $(k = 1, .., N)$ is given by

$$H \equiv \sum_{k=1}^{N} \frac{\mathbf{p}_k^2}{2m} + U(\mathbf{r}_1, \cdots, \mathbf{r}_N), \tag{1}$$

where $\mathbf{p}_k$ is the momentum of the atom k, and the total potential $U(\mathbf{r}_1, \cdots, \mathbf{r}_N)$ is given by

$$U(\mathbf{r}_1, \cdots, \mathbf{r}_N) \equiv \sum_{k=1}^{N} U_s(\mathbf{r}_k) + \sum_{j<k=1}^{N} V(|\mathbf{r}_j - \mathbf{r}_k|). \tag{2}$$

Here, $U_s(\mathbf{r}_k)$ is a single particle potential describing the interaction between the k-th film atom and the substrate, and $V(|\mathbf{r}_j - \mathbf{r}_k|)$ is the pair potential interaction between the j-th and k-th atoms in the film.

The interaction between two Xe atoms is given by a Lennard-Jones potential

$$V(r) = 4\varepsilon \left[\left(\frac{\sigma}{r}\right)^{12} - \left(\frac{\sigma}{r}\right)^{6} \right], \tag{3}$$

where $\varepsilon = 19.83\, meV$, and $\sigma = 4.055\, \mathring{A}$ [14]. The interaction between a Xe atom and the substrate can be described by [15] a substrate potential without internal degrees of freedom

$$U_s(\mathbf{r}_\parallel, z) = U_0(z) + U_1(z) \sum_{\{\mathbf{G}\}} \cos(\mathbf{G}\cdot\mathbf{r}_\parallel), \tag{4}$$

where $\mathbf{r}_\parallel = (x, y)$ are the coordinates of the Xe atom parallel to the substrate, and $\{\mathbf{G}\}$ is the set of the six shortest reciprocal lattice vectors of the substrate. The first term in Eq. (4) describes the mean interaction of the atoms with the substrate, and the second term describes the periodic corrugation potential.

Expressions for $U_0(z)$ and $U_1(z)$ were derived by Steele [15] assuming that the substrate potential $U_s(\mathbf{r})$ is a sum of Lennard-Jones potentials between one film atom and all of the atoms in the substrate. However, summing Lennard-Jones potentials for $U_s(\mathbf{r})$ is not a correct description of a metallic surface interaction with a noble gas atom. The corrugation potential is reduced (from the value found by summing Lennard-Jones potentials) due to electronic screening. For this reason we employ a weaker corrugation potential, as did Cieplak *et al.* in Ref. [10]. The corrugation potential we use is

$$U_1(z) = \alpha e^{-g_1 z^*} \sqrt{\frac{\pi}{2 g_1 z^*}} \left[\frac{A^{*6}}{30} \left(\frac{g_1}{2z^*}\right)^5 - 2\left(\frac{g_1}{2z^*}\right)^2 \right], \tag{5}$$

where $\alpha = 4\pi\varepsilon_{Xe/Ag} A^{*6}/\sqrt{3}$, $z^* = z/a$, $a = 2.892$ $\mathring{A}$ is the lattice constant of the substrate, $A^* = \sigma_{Xe/Ag}/a$, $g_1 = 2/\sqrt{3}$. We calculate the Lennard-Jones parameters $\sigma_{Xe/Ag}$ and $\varepsilon_{Xe/Ag}$ by fitting (i) the position of the minimum of $U_0(z)$ to the distance between a Xe atom in the first layer and the ion cores of the substrate ($z_0 = 3.6\mathring{A}$, from [16]), and (ii) the attractive well depth to the binding energy of one Xe atom to the Ag substrate ($U_0(z_0) = -211 meV$, from [16]). We find $\sigma_{Xe/Ag} = 4.463\,\mathring{A}$ and $\varepsilon_{Xe/Ag} = 13.88$ meV.

Employing Eq. (5) for the substrate potential yields a corrugation amplitude of approximately $3\,meV$. This value is smaller than the corrugation amplitude found using the Steele's potential ($17.4\,meV$) [15]. This last corrugation amplitude leads to slip times two orders of magnitude smaller than those found in experiments. We have been able to reproduce the results for Kr/Au(111) [8,10] employing the above approach.

Our simulations are carried out at an equilibrium temperature of $T = 77.4\,^oK$, and the particles move in a three dimensional box of size $20\,a\times$ $10\,a\sqrt{3} \times 10\,\sigma$. The time scale for

vibrations of the adsorbed film atoms is $t_0 = \sqrt{(m\sigma^2/\varepsilon)} = 3.345\ ps$, with $m = 130.1\ g/mol$. Periodic boundary conditions in the x and y directions are employed along with a hard wall boundary condition in the z direction at the top of the box.

We change the coverage by changing the number of Xe atoms N. We use $60 \leq N \leq 370$. All atoms are initially in the gas phase. The atoms condensed in $250\, t_0$ or less, forming a triangular lattice incommensurate with the substrate fcc(111) surface. A thermostat is used only to establish thermal equilibrium. To calculate the slip time we use two methods:

Method I: An external force (parallel to the substrate surface) is applied to all film particles for approximately 100 t_0. The external force then is removed. This induces an initial center of mass velocity $\mathbf{V}_0$ in the film which decays at later times as $\mathbf{V}_0\, e^{-t/\tau}$. Indeed we find an exponential decay as shown in Fig. 1. The slip-time versus coverage results obtained in this manner are shown in Fig. 2. Because the thermostat was turned off while the decay of the center of mass velocity took place, the temperature rose by at most $13\,^oK$ during this process, which occurred for the largest value for the initial velocities used in these calculations $(0.6\, \sigma/t_0)$.

Method II: In this method no external force is applied at any time. In experiments using QCM [8], one conventionally describes the data by the linear response in the force per unit area δf to an applied substrate velocity δV at complex frequency ζ. This response defines the acoustic impedance of the film, $Z(\zeta) \equiv \lim_{\delta f \to 0}(\delta f/\delta V)$. The Kubo formula for the acoustic impedance has been derived [12] to be

$$Z(\zeta) = -i\zeta\rho_2 \left(1 + i\zeta \int_0^\infty C(t) e^{i\zeta t} dt\right), \tag{6}$$

where $\rho_2 \equiv Nm/A$ is the film mass per unit area A, and the thermal equilibrium autocorrelation function

$$C(t - t') \equiv \frac{< V_x(t) V_x(t') >}{< V_x(0)^2 >} \ . \tag{7}$$

In Eq. (7), $V_x(t)$ is the center of mass velocity of the film in the x direction [17]. The slip time model [12] may be written as a Drude-Darcy law impedance $Z(\zeta) = -i(\zeta\rho_2)/(1 - i\zeta\tau)$, or equivalently, as the autocorrelation function

$$C(t-t') = \exp\left(-\frac{|t-t'|}{\tau}\right). \tag{8}$$

Equation (8) is the basis of the second method for calculating τ. The thermal average in Eq. (7) is calculated performing an average over a time t_{tot}

$$< V_x(t)V_x(t') >= \frac{1}{t_{tot}} \int_0^{t_{tot}} V_x\,(t+s)\, V_x\,(t'+s)\, ds. \tag{9}$$

In Fig. 2, the values of the slip time as a function of film coverage are shown for the two methods described above. The two methods yield results which are qualitatively similar to each other and to previous experiments.

We find a minimum followed by a sharp rise in the slip time for coverages near one monolayer. The minimum in τ corresponds to the uncompressed monolayer (see Fig. 2). We are able to observe directly in the simulations a compression of the monolayer when the coverage varies from 0.0563 atoms/$\AA^2$ to 0.0594 atoms/$\AA^2$. The interparticle average spacing at these coverages are respectively: 4.53 $\AA$ and 4.4 $\AA$. These values are very close to those reported experimentally by Unguris et al. [19] (4.52 $\AA$ and 4.39 $\AA$ for the uncompressed and fully compressed monolayer).

The structure factor

$$S(\mathbf{Q}) \equiv \frac{1}{N} < \sum_{i,j}^{N} \cos\left(\mathbf{Q}\cdot(\mathbf{r}_i - \mathbf{r}_j)\right) > \tag{10}$$

has also been calculated. In Fig. 3 we show the Bragg peaks in the $\mathbf{Q} = (Q_x, Q_y, 0)$ plane for different coverages: submonolayer, slightly below uncompressed monolayer and compressed monolayer coverages. The Bragg peaks for the larger slip times (compressed monolayer) are sharper than the Bragg peaks for the smaller slip times (submonolayer and slightly uncompressed monolayer). Thus, the lattices corresponding to small slip-times have more disorder than lattices with large slip-times.

Persson and Nitzan [11] have recently calculated friction for the present system using molecular dynamics in a model that includes a Langevin thermostat, which they identify with the effect of electronic excitations in the substrate. This thermostat uses unequal

damping constants in directions parallel and perpendicular to the sliding direction (i.e. $\eta_{\|} = 6.2 \times 10^8\,\mathrm{sec}^{-1}$ and $\eta_{\perp} = 2.5 \times 10^{11}\,\mathrm{sec}^{-1}$.) They find a resulting friction constant $\eta_{tot} \approx 6.32 \times 10^8\,\mathrm{sec}^{-1}$ in their simulations, for a monolayer coverage. Assuming $\eta_{tot} = \eta_{\|} + \eta_{phon}$, one finds that the phonon contribution to friction $\eta_{phon}/\eta_{total} = 0.02$. Thus there appears to be a significant reduction in η_{phon} due to the presence of the electronic damping $\eta_{\|}$. We have performed simulations using the substrate potential of Eqs. ([4]-[5]) with the same Langevin thermostat and damping constants as Persson and Nitzan. We find, for a monolayer coverage ($0.0563\ atoms/\AA^2$), that $\eta_{total} = 2.45 \times 10^9\,\mathrm{sec}^{-1}$ and $\eta_{phon} = 1.83 \times 10^9\,\mathrm{sec}^{-1}$, so that $\eta_{phon}/\eta_{total} = 0.75$. Thus, although the suppression of the phonon contribution to friction is significant, it is not as drastic as that reported in ref. [11].

In conclusion, we have performed molecular dynamics simulations of Xe/Ag(111) in a thermostat-free environment. We have been able to qualitatively and semi-quantitatively reproduce the experimental data [6] by means of two independent methods which simulated sliding speeds, which are at least three orders of magnitude apart. In particular, our simulation reproduces the distinctive dip in the submonolayer regime found in experiment. This result, combined with the fact that the electrical surface resistivity was found to be nearly constant in this regime [7] suggests that the phonon contribution dominates over the electron contribution for this system. The fact that the simulations yielded comparable slip times for greatly varying sliding speeds demonstrate the linearity in velocity of the friction governing this system.

This work has been supported in part by the NSF, Grant No. DMR9204022 and by the USD of Energy grant No. DE-FG02-96ER45585. We would like to thank Prof. H. E. Stanley for his aid. One of us (M. S. T.) would like to thank H. A. Makse for useful discussions.

REFERENCES

[1] F. P. Bowden and D. Tabor, *Friction and Lubrication* (Methuen, London, 1967); J. F. Archard, Proc. R. Soc. London Series. **A 243**, 190 (1957).

[2] D. Dowson, *History of Tribology* (Longman, London, 1979).

[3] J. B. Sokoloff, Phys. Rev. B **42**, 760,6745(E) (1990); Phys. Rev. **B47**,6106 (1993); Wear **167**, 59 (1993); Phys. Rev. Lett. **71**, 3450 (1993); Phys. Rev. **51**, 15573 (1995).

[4] J. B. Sokoloff, Phys. Rev. B **52** 5318,(1995).

[5] E. T. Watts, J. Krim, and A. Widom, Phys. Rev. B **41**, 3466 (1990); A. Widom and J. Krim , Phys. Rev. E **49**, 4154 (1994).

[6] C. Daly and J. Krim, Phys. Rev. Lett. **76**, 803 (1996).

[7] A. Dayo and J. Krim, Proc. 8^{th} International Conference on Vibrations at Surfaces, Birmingham, England, June, 1996, Surf. Sci. in press.

[8] J. Krim, D. H. Solina, and R. Chiarello, Phys. Rev. Lett. **66**, 181 (1991); J. Krim, Comments Cond. Matt. Phys. **17**, 263 (1995).

[9] B. N. J. Persson and A. I. Volokitin, J. Chem. Phys. 103, 8679 (1995).

[10] M. Cieplak, E. D. Smith, and M. O. Robbins, Science **265** 1209 (1994); Phys. Rev. B **54**, 8252 (1996).

[11] B. N. J. Persson and A. Nitzan, Surf. Sci. **367**, 261 (1996).

[12] J. Krim and A. Widom, Phys. Rev. B **38**, 12184 (1988).

[13] R. Kubo, M. Toda, N. Hashitsume *Statistical Physics II: Nonequilibrium Statistical Mechanics*, sec. ed. (Springer-Verlag, Heidelberg, 1995).

[14] J. G. Dash, *Films of Solid Surfaces* (Academic Press, London, 1975).

[15] W. Steele, Surf. Sci. **36**, 317 (1973).

[16] G. Vidali, G. Ihm, H.Y. Kim, and M. Cole, Surf. Sci. Reports **12**, 133, (1991).

[17] In our simulations we take V_x as the center of mass velocity minus its mean $< V_x >$. Subtracting the mean center of mass velocity is a standard technique that, in a molecular dynamics simulation, ensures that the correlation goes to zero at long times [18].

[18] J. M. Haile, *Molecular Dynamics Simulation: Elementary Methods* (Wiley, New York, 1992).

[19] J. Unguris, W. L. Bruch, E. R. Moog, and M. B. Webb, Surf. Sci. **87**, 415 (1979).

FIGURES

FIG. 1. Typical decay of the center of mass velocity (in units of σ/t_0) after applying the external force. After the force and thermostat are turned off, the velocity decays; and this portion of the graph is fitted to an exponential curve as predicted by the linear friction force law to obtain the slip time (method I).

FIG. 2. Slip time τ (in units of sec.) versus coverage (in units of number of particles per $\mathring{A}^2$) for the two methods used. (a) Method I. (b) Method II. Solid lines in both figures are three of the experimental curves from Ref. [6], included for comparison. There is qualitative and quantitative agreement with experiment. Both methods reach a minimum near 0.0563 atoms/$\mathring{A}^2$.

FIG. 3. Bragg peaks for (a) a submonolayer coverage, 0.040 atoms/$\mathring{A}^2$, (b) slightly below uncompressed monolayer coverage, 0.0538 atoms/$\mathring{A}^2$, and (c) the compressed monolayer coverage, 0.0594 atoms/$\mathring{A}^2$.

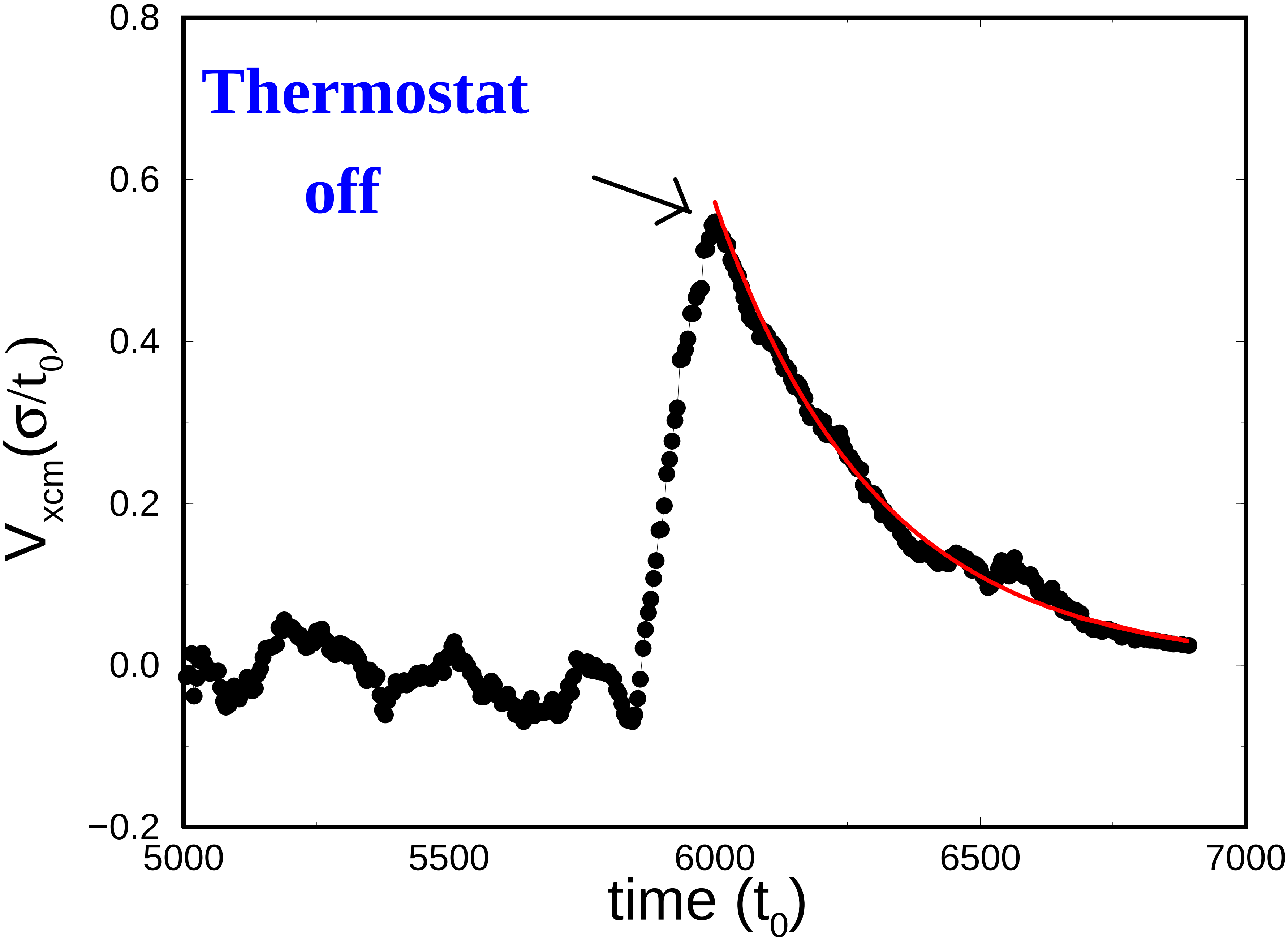

Thermostat
off
0.8
0.6
0.4
0.2
0.0
−0.2
5000
5500
6000
6500
7000
$V_{xcm}(\sigma/t_0)$
time (t_0)

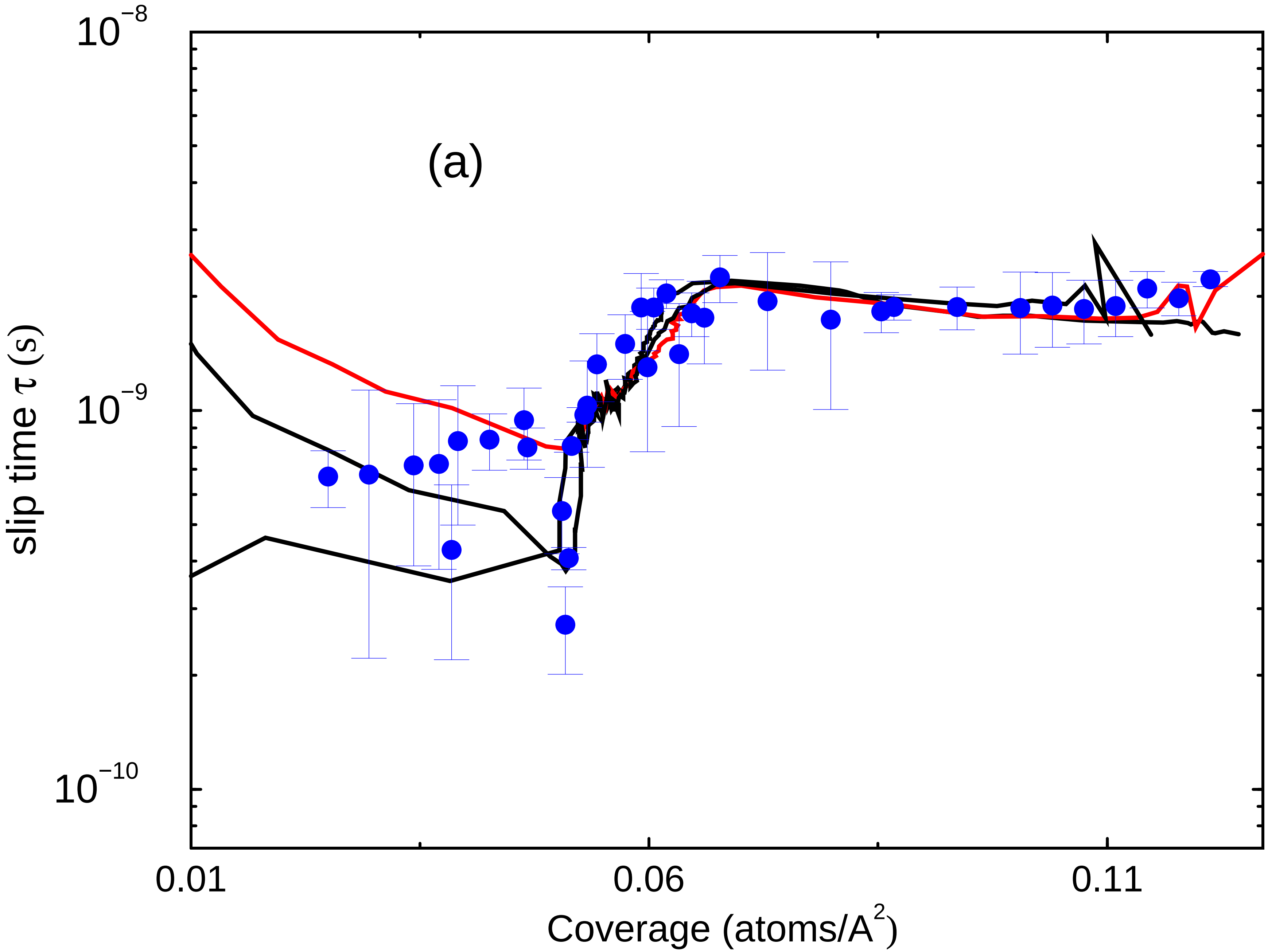

(a)
10^{-8}
10^{-9}
10^{-10}
slip time τ (s)
0.01
0.06
0.11
Coverage (atoms/A^2)

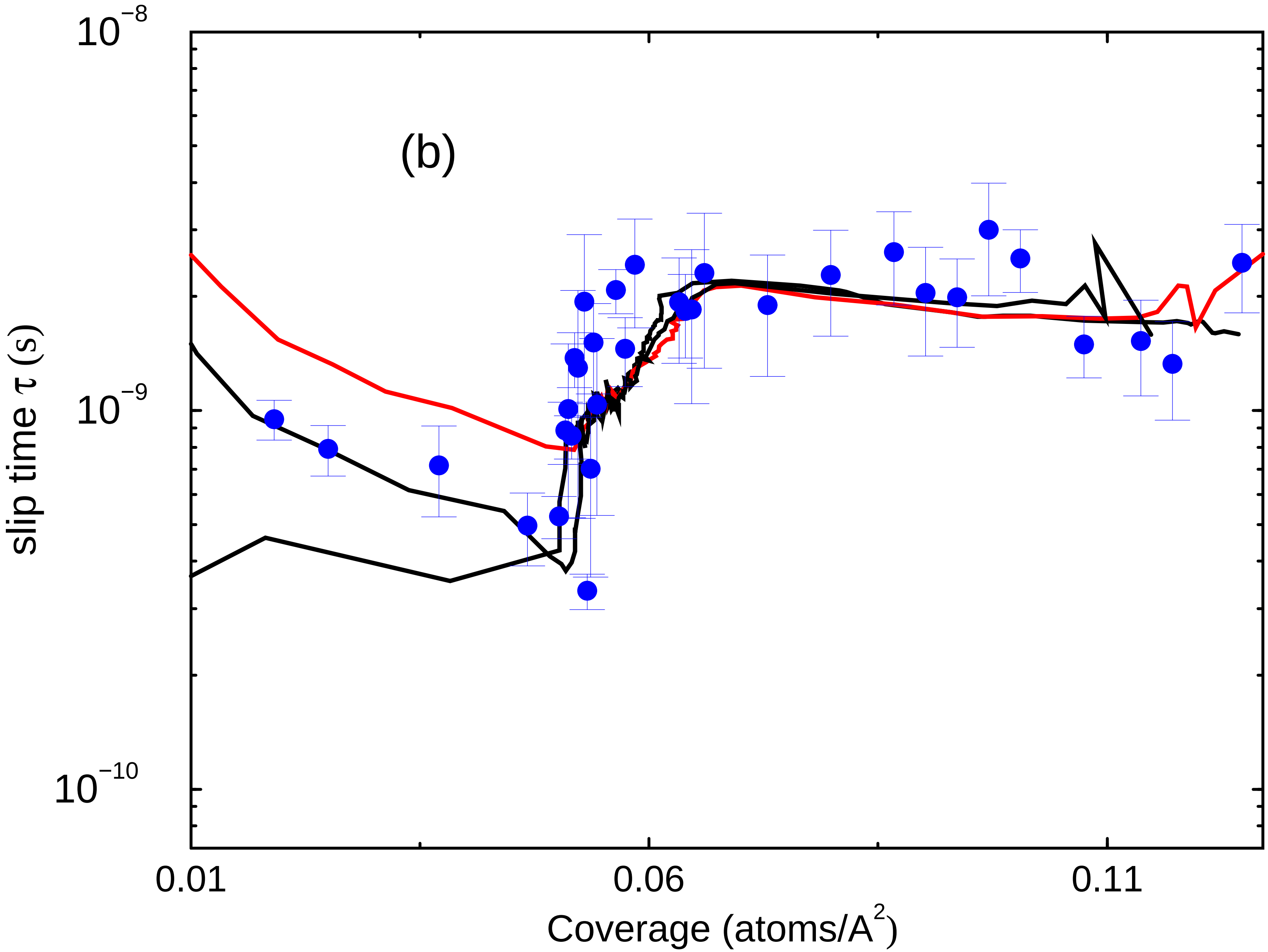

(b)
slip time τ (s)
10^−8
10^−9
10^−10
0.01
0.06
0.11
Coverage (atoms/A^2)

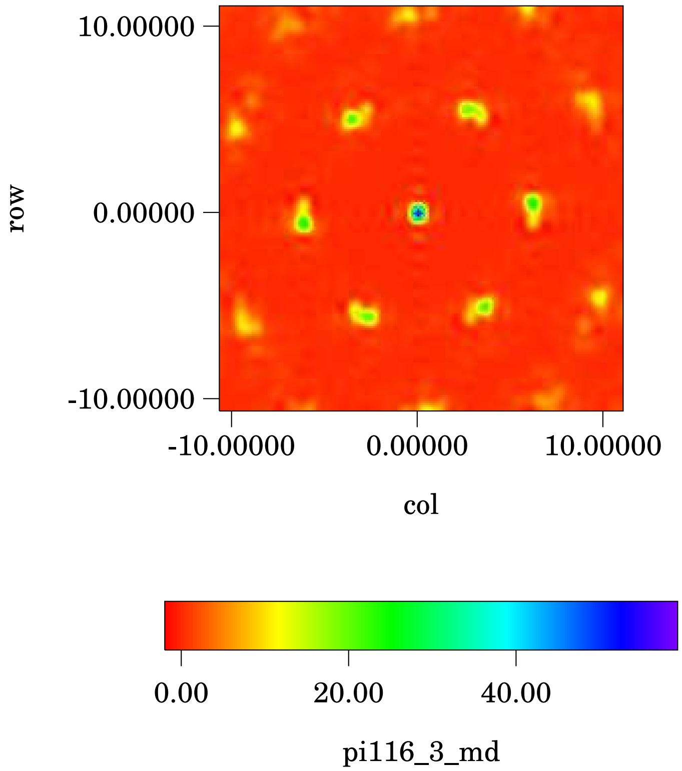
10.00000
0.00000
-10.00000
row
-10.00000
0.00000
10.00000
col
0.00
20.00
40.00
pi116_3_md

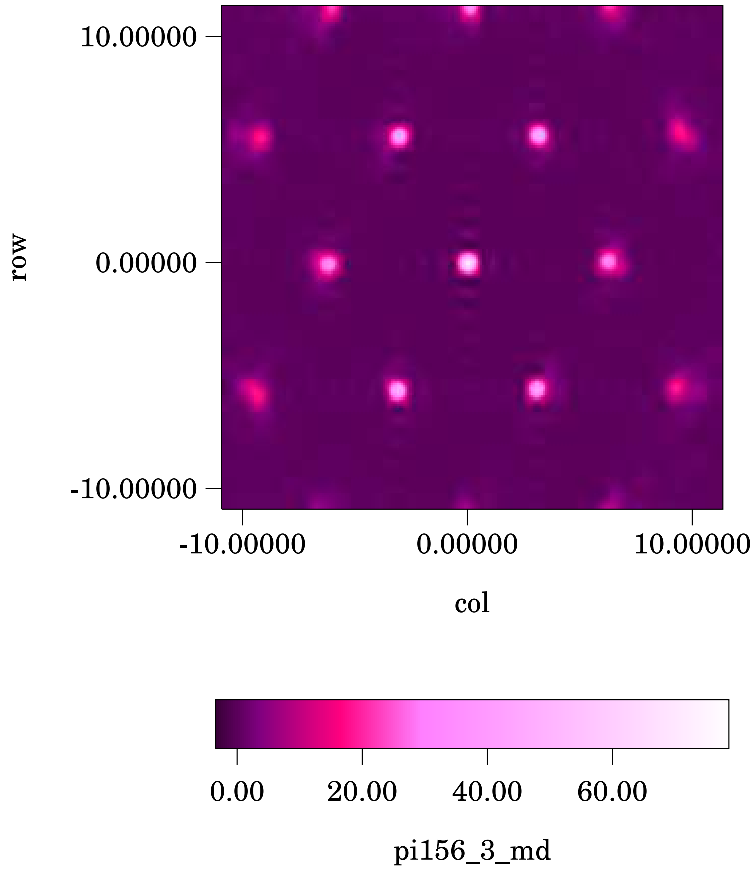
10.00000
0.00000
-10.00000
row
-10.00000
0.00000
10.00000
col
0.00
20.00
40.00
60.00
pi156_3_md

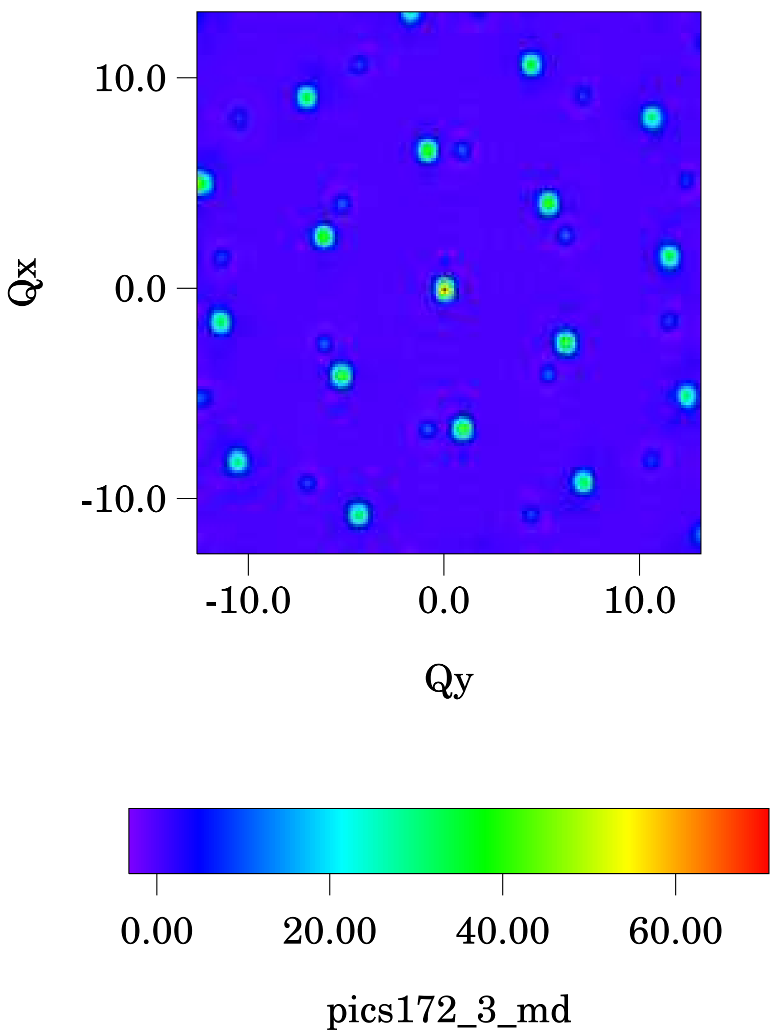

Qx
10.0
0.0
-10.0
-10.0
0.0
10.0
Qy
0.00
20.00
40.00
60.00
pics172_3_md